JOINT EUROPEAN TORUS JET

JET-R(85)03

P.H. Rebut, M. Hugon, S.J. Booth, J.R. Dean, K.J. Dietz, K. Sonnenberg
and M.L. Watkins

Low–Z Material for Limiters and Wall Surfaces in JET: Beryllium and Carbon

Low–Z Material for Limiters and Wall Surfaces in JET: Beryllium and Carbon

P.H. Rebut, M. Hugon, S.J. Booth, J.R. Dean, K.J. Dietz, K. Sonnenberg and M.L. Watkins

JET Joint Undertaking, Culham Science Centre, OX14 3DB, Abingdon, UK

ABSTRACT

It is proposed to use in JET a single low-Z material for the belt limiters and the walls to reduce impurity radiation losses to the lowest level. The only practical materials are graphite and beryllium. Their relative merits are compared in this paper. Graphite has better thermomechanical properties than beryllium, but simulation experiments on beryllium carried out at Sandia National Laboratory and in ISX-B have proved these properties sufficient for the belt limiters. Recent measurements indicate that beryllium retains 2–3 times less hydrogen than graphite. The ISX-B experiments have shown that beryllium has an excellent gettering action also. The main drawback of beryllium is the toxicity of its dust, but the control of beryllium dust is well within standard industrial techniques. It is concluded that beryllium offers the best prospects as a material for the JET belt limiters and walls.

I INTRODUCTION

The study of plasma-wall interactions is one of the four main aims of the JET experiment as outlined in Ref. /1/. To reach the near-reactor conditions aimed at in JET and hence to justify the eventual use of tritium, it will be necessary to solve the plasma-wall problem to the extent that both the radiation and the dilution effects in the plasma core are sufficiently small.

1. Belt limiters

In the next phases of the project additional heating will be applied progressively to increase the power input into the torus from the present ohmic level of 2-3MW up to $\sim$40MW. To take this increase in power the present discrete, uncooled, carbon limiters will be replaced by two continuous, radiation-cooled, "belt" limiters mounted above and below the mid-plane on the large major radius part of the vacuum vessel (see Fig. 1). The RF antennae will be mounted between these limiters. The design is such that the main plasma-wall interaction takes place on the edges of specially shaped tiles on the belt limiters with a similar arrangement for the antennae protection.

2. Cool plasma mantle or high temperature edge

There are two extreme scenarios for the operation of JET:

- impurities of medium-Z are present in the outer regions in sufficient quantity so that a large fraction of the power input is radiated by the "cool plasma mantle". This mode is probably inescapable if the limiter is made of middle-Z material, (e.g. nickel), or if the Inconel walls are exposed to the plasma. The "cool plasma mantle" mode has the advantage of reducing the power load on the limiters and of being self-regulating.

- the alternative mode of operation is one in which the major part of the power input is deposited on the limiters with only a small fraction radiated. To achieve this, the impurities must have a very low Z ($Z < 8$). This could be obtained, if the plasma only interacts with a very low-Z material (limiters, walls, antennae,....). In this case, it would still be possible to operate in the "cool plasma mantle" mode by controlled injection of elements, such as argon, into the plasma. Clearly, this low-Z solution gives maximum flexibility in permitting a study of both operational modes.

3. Consequences of radiative losses

To reach ignition conditions, radiative power losses due to impurities must be only a limited fraction (<50%) of α-particle heating. When the impurities are fully ionised, bremsstrahlung losses impose an upper limit on Z_{eff} (typically $Z_{eff} < 6$ for $Te \cong 15keV$), which defines a maximum impurity concentration in the plasma centre.

Although the global power balance in a tokamak is fundamental, radiative losses at the edge may play a critical role in plasma stability and confinement.

Disruptions impose a major limitation on tokamak performance: they impose limits on plasma parameters such as the maximum electron density and the lowest q-values attainable and, as a consequence, on the product $n\tau$; they limit machine performance by the forces induced on the vacuum vessel and coils, and by thermal stresses on limiters and walls. With increases in plasma current and, probably, in β, disruptions occur faster, since the plasma requires a more important readjustment of the vertical field to stay in equilibrium. As the densities reached with additional heating may exceed the density limit with ohmic heating, termination of the discharge may well induce further disruptions, once additional heating is stopped. Experimentally, it has been found that disruptions are sensitive to plasma edge conditions (impurities, radiation, wall carbonisation on JET). In a theoretical model /2/, it is predicted that disruptions due to the high density limit could be suppressed by strongly decreasing external losses (radiation and recycling).

Assuming that disruptions could be controlled, thermal collapse might occur, if the losses in the outer plasma region exceed the total input power. The power balance permits the derivation of an upper density limit in the edge, which depends on the nature of the impurities and on the total input power /3/.

"H-mode" properties are interesting to improve the energy confinement time. "H-mode" is due to the emergence of a zone close to the separatrix in the outermost plasma layer, where the confinement is good (classical?). This allows a strong temperature gradient at the edge and higher plasma performance. Under these conditions, impurity accumulation is currently observed: e.g. iron in ASDEX, nickel, chromium and titanium in PBX. When their concentration becomes too large, most of the plasma energy is lost by radiation or charge exchange. This eventually returns the plasma to the "L-mode".

This discussion clearly indicates the necessity of limiting the radiative losses right to the outermost plasma zone. Only impurities with very low atomic number could be tolerated at relatively large concentrations at the plasma edge. The main advantages of having only impurities of very low atomic number Z can be summarised as follows:

- ions are fully stripped and therefore line radiation loss is suppressed at temperatures of a few keV; this is true for $Z \lesssim 10$ at T=3keV;

- the tolerable concentration can be relatively large, since the critical impurity concentration for inhibiting ignition is proportional to Z^{-1} (see Fig. 2);

- for a stationary state, if the ion confinement is close to classical, the impurity density may strongly peak in the plasma centre. The maximum magnitude decreases, as Z decreases.

4. Importance of having a single material for the limiters and the walls

In a tokamak, the main sources of impurities are the limiters and the wall. Their magnitude is generally enhanced by additional heating.

Deposition of wall materials on the limiters and the inverse process are observed in all tokamaks. In JET, the graphite limiters have been covered by the constituents of the wall (in particular nickel) with an average layer of up to 50 monolayers; in ISX-B, the beryllium limiter has been covered with chromium, evaporated on the walls for a prior gettering experiment; in TFR, molybdenum has been deposited on the walls when molybdenum limiters were used and in ISX-B beryllium has covered a part of the wall after the melting of the beryllium limiter. This indicates that is is practically impossible to segregate limiter and wall materials. When different materials are used, it is difficult to know the composition of the materials in contact with the plasma and the effect of the mixture (e.g. carbides, when graphite is used).

5. Present low-Z experiments

In JET, recent experiments have been carried out with four discrete graphite limiters (total area $1.3m^2$) and power input in the range 1-3MW. In order to suppress high-Z impurities and to observe the effect of discharges with low radiation at the edge, the walls have been carbonised by glow discharge cleaning in mixtures of methane and hydrogen. After carbonisation, the main features of the discharges are:

- the nickel content is strongly reduced. Typically, for a relatively high density pulse ($\bar{n}_e = 3 \times 10^{19} m^{-3}$), the measured impurity concentrations relative to the central electron density are 2.5%, 1% and 0.015% for carbon, oxygen and nickel, respectively. These concentrations give $Z_{eff} = 2.4$ and $n_D/n_e = 0.77$;

- the power radiated by impurities is about 50% of the ohmic power input;

- the release of hydrogen from limiters and wall makes density control difficult during the current pulse.

The trend of using a single low-Z material in JET has been followed in TEXTOR, where heavy wall carbonisation has allowed the injection of 1MW RF heating without disruption, whereas previously it had been limited to 100kW.

6. Ideal limiter and wall requirements

Ideally, the limiter and wall material should have the following properties:

- very low atomic number;
- negligible porosity;
- high melting point;
- large thermal conductivity;
- good resistance against thermal shock;
- low erosion through sputtering or chemical effects;
- low hydrogen retention and low chemical affinity with hydrogen;
- strong affinity to oxygen (gettering action).

7. Summary

These considerations all tend to the conclusion that using a single low-Z material for limiters and walls provides a solution to reduce impurity radiation losses to an acceptable level. The only materials which meet a sufficient number of the above criteria are beryllium and carbon. In this paper, the relative merits of the two materials are discussed. Section II sets out transport code predictions, and thermomechanical and physical properties are compared in Section III. To clarify these points, a beryllium limiter experiment has been undertaken in ISX-B at ORNL, USA; the results of this experiment are reported in Section IV. Due to the toxicity of beryllium, precautions required when entering the JET vacuum vessel containing beryllium are discussed in Section V.

II THE EFFECT OF LOW-Z LIMITER AND WALL MATERIAL ON THE APPROACH TO IGNITION

1. Introduction

Transport code predictions for tritium operation in JET at the full planned power are presented with the aim of allowing conclusions to be drawn regarding the choice of limiter material and the effect of dissimilar materials also being present.

Several impurity contaminants are likely to be present in JET (e.g. nickel deposits from the wall and radiofrequency antennae onto beryllium or carbon limiters, intrinsic oxygen, injected neon). Two ideal situations are considered, classified as "all low-Z" (the limiter and wall are of the same low-Z material, either beryllium or carbon) or "mixed-Z" (the limiter is of low-Z material, the wall is nickel and is assumed not to contaminate the limiter). The oxygen level is assumed to be sufficiently low that gettering is not needed. 100% recycling of the hydrogen isotopes is assumed. Only physical sputtering of impurities is taken into account.

Earlier calculations comparing the use of beryllium and carbon (and nickel) as limiter materials /5, 6/ used a variety of plausible transport models, since no single model existed then to describe tokamak plasmas in all detail.

The results of ohmic operation in JET have allowed some of the uncertainties in these models to be removed, allowing the identification of the most appropriate transport model then used (Section II.2). The results of these calculations are reviewed in Section II.3.

These calculations have also been updated, taking account of the results of JET operation to date (Sections II.4 and II.5).

2. Model assumptions for the most relevant cases in Refs./5,6/

The form of the ICARUS transport model used can be found in /5,6/.

The most important features for the present study are: ALCATOR/INTOR anomalous electron thermal losses ($\chi_e = 5 \times 10^{19}/n_e$); anomalous diffusive ($D = \frac{1}{4}\chi_e$) and inward convective ($V = 2rD/a^2$) particle fluxes; neoclassical values for the ion thermal losses and the electrical resistivity (including trapped particle corrections); transport in the scrape-off layer is characterised by the parallel confinement time, $\tau_{/\!/} = L/V$ (where L is the effective connection length taken to be πRq and V is the effective ion flow speed); impurities are produced at the limiter by sputtering by charged particles, and at the wall by charged particles and charge-exchanged neutrals (self sputtering is included); coronal radiation losses are assumed.

This model is applied to a circular cross-section torus with the same volume as the JET configuration (limiter radius, $a_L = 1.62$m; wall radius, $a_W = 1.72$m; major radius R=2.96m).

The heating sources correspond to those for the full planned power of JET (Phase IV operation with a toroidal field of 3.45T) and comprise the sum of:

a. ohmic heating with a current of 4.8MA from time, t=0s;
b. injection of neutral deuterium at a power level of 10MW at an energy of 160keV (a total power of 17.25MW including the fractional energy components) from time, t=0s;
c. a uniform ion heating profile of about 0.1MWm^{-3} to represent some form of radiofrequency heating at an effective level of 15MW within the limiter radius from time, t=1s; and
d. alpha particle heating by plasma-plasma and beam-plasma interactions assuming a 50:50 mixture of deuterium and tritium.

A mean deuterium/tritium starting density of $4.4 \times 10^{19} \text{m}^{-3}$ is assumed.

3. Results of the most relevant cases in Refs. /5,6/

The results of simulations presented in /5,6/ for all low-Z and mixed-Z cases are summarised in Table I at a time of 3s, when the central ion temperature has, in most cases, reached its maximum value.

In terms of plasma performance for these high density cases (central deuterium/tritium densities $\sim 10^{20} m^{-3}$), there is little to choose between beryllium and carbon as the limiter material for either the all low-Z or the mixed-Z cases. The central temperatures are quite high (9-10keV) and a modest alpha power results (3-6MW).

The main difference arises between the all low-Z and the mixed-Z cases in the level of limiter erosion and radiated power. With all low-Z cases, the edge temperature, the power flux to the limiter and the limiter erosion are all high, and the radiated power is low. With mixed-Z cases, the edge temperature, the power flux to the limiter and the limiter erosion are all low, and the radiated power is high.

4. Updated model assumptions

A result of ohmic operation in JET has been the refinement of the basic transport model, the most important changes being an anomalous electron thermal diffusivity that is one-half of the ALCATOR/INTOR value ($\chi_e = 2.5 \times 10^{19}/n_e$) during the ohmic phase of operation; during additional heating the value of the ohmic diffusivity is increased by a factor of two and held independent of density; twice the neoclassical ion thermal losses; and a particle diffusion coefficient, $D = 0.5 m^2 s^{-1}$.

The model is applied to a full aperture, D-shaped JET plasma (limiter radius, $a_L = 4.21m$, wall radius, $a_W = 4.32m$, major radius, $R = 2.96m$ in the horizontal mid-plane; ellipticity=1.6; triangularity=0.25).

The heating sources are as indicated in Section II.2, except:

a. ohmic heating with 3.8MA starts at time, t=0s;
b. the injection of neutral deuterium from time, t=1s at a power level of 10MW at an energy of 160keV (a total power of 15MW with the present best estimates of the fractional energy components) is modelled more accurately by a multiple pencil beam description which takes full account of the neutral beam injection and tokamak plasma geometries;
c. the radiofrequency heating starts at time, t=2s.

A lower mean deuterium/tritium starting density of $2.2 \times 10^{19} m^{-3}$ is assumed, consistent with the density limit observed so far in ohmic operation.

5. Results of updated calculations

The results of the more recent calculations are summarised in Table II at a time of 3s. Most differences with the previous calculations may be attributed to the assumed lower ohmic starting density.

In terms of plasma performance for these low density cases (central deuterium/tritium densities $\sim 6 \times 10^{19} m^{-3}$ at 3s), there is still little to choose between beryllium and carbon as limiter material. The central temperatures (10-13keV) are a little higher than those obtained previously, but the alpha power is lower ($\sim$2MW) as a result of the lower density. The limiter erosion and the low-Z concentrations are higher.

The main difference from the earlier calculations arises with the mixed-Z cases, in which, at low plasma density, insufficient nickel accumulates in the low density edge region to radiate more than 50% of the input power. The edge temperature, the power flux to the limiter and the limiter erosion are therefore high, similar to the corresponding all low-Z cases.

6. Conclusions

With the models examined (which assume a negligible oxygen level, 100% recycling of hydrogen isotopes and only physical sputtering of impurities) these calculations indicate there is little to choose between beryllium or carbon as the limiter material for JET. This result is independent of the effective wall material, the plasma density and the heating model.

Systems comprising all low-Z material lead to high edge temperatures, high power flows to the limiter, high limiter erosion and low impurity radiation for both low and high plasma density.

Low-Z impurity levels remain tolerably low (despite the large limiter fluxes and the assumed transport model which peaks impurities on axis) because redeposition on the limiter and modest transverse transport into the bulk plasma ocurs. This model is appropriate for present ohmic discharges in JET.

Systems comprising mixed-Z materials are shown to be much more sensitive to changes in, for example, the plasma density. At low density, the edge temperature, the power flow to the limiter and the limiter erosion are all high and the impurity radiation is low, similar to the corresponding all low-Z cases. At high density, however, the edge temperature, the power flow to the limiter and the limiter erosion are all low and the impurity radiation is high.

III COMPARISON OF BERYLLIUM AND GRAPHITE PROPERTIES

1. Physical properties

Table III compares some of the physical properties of beryllium and graphite.

Properties favouring beryllium as a limiter material are its low Z value and its negligible porosity. However, its relatively low melting point makes it more vulnerable to disruptions (see Section 2c).

Graphite has the advantage of not melting but sublimating and exhibits a larger heat of sublimation. Its main disadvantage is its relatively large porosity, which could generate a serious outgassing problem if a complete coverage of the inner wall with graphite is envisaged.

2. Thermal and mechanical resistance

a. During normal plasma pulses

To compare the effects of thermal stresses on different materials, $\sigma_B/E.\alpha.\Delta Ts$ is usually quoted as a figure of merit. For short temperature pulses, $\Delta T_s \cong (c.k)^{-\frac{1}{2}}$, the figure of merit is about 5 times larger for graphite than for beryllium (see Table III). However, this factor of 5 is likely to be an overestimate, since it does not take into account the large ductility of beryllium (particularly at high temperature).

To test the thermomechanical properties of beryllium for suitability as the JET belt limiters, thermal fatigue experiments have been undertaken:

- in the ISX-B tokamak at Oak Ridge, where a beryllium limiter was subjected to short high power heat pulses (2500 W/cm^2 for 0.3s) (see Section IV.2);

- in an electron beam facility at Sandia National Laboratory, where beryllium samples were exposed to heat loads similar to those that would be experienced in JET (300 - 450W/cm^2 for 10s). A first set of samples has survived 10000 cycles of 300W/cm^2 without structural damage. Microcrack formation was observed after about 3000 cycles. These cracks widened in the course of the experiment and additional microcracks appeared. The range of crack growth did not exceed 5mm and is in good agreement with the range of plastic deformation obtained from elastic-plastic finite element calculation. Thermal fatigue tests at higher heat loads (450 W/cm^2 for 10 s) are being performed, but from the elastic-plastic calculations no dramatic change in crack formation is expected.

Apart from thermal stresses, the heat load may also be limited by excessive temperatures at the limiter surface. This would result in very large evaporation of the limiter surface material and in intolerable concentrations of this material in the plasma. Surface temperatures of the JET belt limiters have been calculated for an average heat load of 300W/cm^2 and different peak loads. They are compared in Table IV for beryllium and carbon materials. The values shown in Table IV are steady state temperatures after about 10 pulses with a duration of 10s and at a repetition rate of 20mn.

In the case of beryllium, a conservative upper limit for the heat load on the limiter can be defined by the surface temperature at which the evaporation rate is about a factor of 10 lower than the sputtering rate* (see Fig. 3): it is about 440 W/cm^2. Assuming that the scrape-off layer thickness varies by less than a factor of 4, it is possible to shape the belt limiter so that the local peak loads are about 60% higher than the average load.

---

*As the sputtering rate has been calculated for the maximum energy of the particles impinging on the limiter (E=900eV), it is a lower limit. For lower energies (300<E<900eV), the particle flux would be larger for the same power flux and the sputtering yield would also be higher.

Taking for the peak loads 440W/cm^2, the average power flux on the belt limiter is 275W/cm^2, which corresponds to a total load of about 40MW. Surface melting is expected at heat loads of 600W/cm^2 for 10 s. The margin between 440 and 600W/cm^2 may be considered as a safety factor of 1.4 for the beryllium belt limiter.

b. Damage by runaway electrons

In this case, the temperature increase is not determined by the thermal conductivity, but by the specific heat. The figure of merit then becomes $\sigma_B.c/E.\alpha$. The value for graphite is about 5 times higher than for beryllium, but this comparison does not take into account the high ductility of beryllium.

So far, damage by runaway electrons has been observed for graphite only /7/. It shows a laminar fracture about 1 mm deep. Similar damage is expected for beryllium, since the heat effected zone (determined by the density of the material) should be the same for both materials.

It should be noted that, in contrast to Inconel in JET, beryllium is not expected to melt under runaway electron impacts. The temperature increase resulting from volumetric energy deposition should be only about 500°C in beryllium due to its low density.

c. Damage by disruptions

Only theoretical calculations are available. For example, disruptions depositing an energy density of 1000J/cm^2 over a period of 5ms are expected to evaporate a 100µm thick layer and to melt an additional layer of about 100µm thickness for beryllium. Evaporation to a depth of only 50µm is expected for graphite due to its higher heat of sublimation. Since it is not clear whether the melted layer of beryllium will be stable against eddy current forces /8/ or internal pressure, erosion could be 2 to 4 times higher for beryllium than for graphite.

3. Sputtering

For graphite, sputtering depends strongly on temperature: it is enhanced by chemical effects around 550°C and by radiation damage at higher temperatures /9/. By contrast, for beryllium, the sputtering exhibits only a weak temperature dependence /10/. At the temperatures indicated in Table IV, yields on sputtering by hydrogen and deuterium are lower for beryllium than for graphite.

4. H - recycling

a. Retention and release of injected (≧50eV) hydrogen

During plasma build-up, a fraction of the hydrogen impinging on the belt limiter is trapped in a thin surface layer. When the limiter is heated up by the plasma pulse, part of the trapped hydrogen is thermally released. The amount of hydrogen trapped and released during the pulse depends on the limiter material, on its temperature when implantation occurs and on the energy of the impinging hydrogen.

Most of the experimental studies for hydrogen retention in materials as a function of temperature have been made using the following procedure: after hydrogen implantation at 20°C, the hydrogen content is measured for different temperatures of the material. The data obtained for beryllium and graphite are shown in Fig. 4 (full symbols). A comparison is only possible for implantation at 1500eV. At room temperature, the amount of trapped hydrogen is larger by nearly a factor of 2 in graphite than in beryllium. However, the release of hydrogen upon heating is quite different for both materials. Beryllium exhibits two release stages at 200 and 480°C, whereas for graphite hydrogen is released in a single stage at about 700°C/11/. These measurements indicate that after heating above 300°C hydrogen retention is larger by more than one order of magnitude in graphite than in beryllium.

However, the above results do not reflect the reality. In JET, while hydrogen implantation occurs, the temperature of the belt limiter will be about 300°C and will further increase after additional heating is applied (see Table IV). Recent measurements for hydrogen retention in beryllium as a function of the implantation temperature /12/ are compared with the data for graphite in Fig. 4 (open symbols). In the case of implantation at 1500eV, beryllium retains less (factor 2-3) hydrogen than graphite above 200°C. This reflects the fact that hydrogen is thermally released from beryllium at a lower temperature than from graphite. As the hydrogen retention curves for beryllium seem to present the same type of behaviour as a function of implantation temperature for different energies, the factor of 2-3 is assumed to be valid for lower energies also.

Hydrogen release by the belt limiter in the case of graphite has been estimated in two different ways: (i) from isotope exchange experiments in JET (e.g. Pulse No. 2751); (ii) by a simple calculation which assumes an electron temperature of 100eV in front of the limiter and a maximum value of 300eV for the sheath potential. Both estimations indicate that an increase in average density of 2 to $8 \times 10^{19} m^{-3}$ is expected during the discharge as soon as the limiter temperature exceeds 800°C (see Table IV). This might make density control difficult in JET.

b. No reliable data are available for diffusion, solubility and surface recombination of hydrogen for beryllium and graphite.

5. Reaction with oxygen

Carbon combines with oxygen to give volatile oxides (carbon dioxide and carbon monoxide). In contrast, beryllium forms a non volatile, thermally extremely stable oxide. This property allows the use of beryllium as an oxygen getter, as shown in the experiments performed in UNITOR and ISX-B (see Section IV).

6. Conclusions

Although the thermomechanical properties of beryllium are not as good as those of graphite, simulation experiments have proved them sufficient for JET application. However, compared to graphite, beryllium has a lower Z value, has a negligible porosity, retains less hydrogen at high temperatures, has a lower yield on sputtering by hydrogen and can be used as a getter.

IV RESULTS OF THE ISX-B BERYLLIUM LIMITER EXPERIMENT

Before using beryllium as a limiter material in JET, it was decided to study the behaviour of smaller tokamaks equipped with beryllium limiters. A preliminary experiment was carried out in a small tokamak, UNITOR, in Dusseldorf. After the first encouraging results, a more comprehensive set of tests was carried out in ISX-B in Oak Ridge. A brief summary of the ISX-B experimental results /13/ is given in this section.

1. Experiment specifications

The objectives of the experiment were to study in a beam heated machine the behaviour of plasmas in the presence of a beryllium limiter and to investigate the mechanical suitability of this material under high heat loads and high particle fluences.

The experiment was specified for a deuterium fluence of about 10^{22} ions/cm^2 to the limiter. This corresponded to 3000 beam-heated discharges. The limiter was designed to experience a surface temperature rise of 600°C per discharge. The resulting power flux was 2.5kW/cm^2 during a plasma pulse of 0.3s.

To simulate JET conditions, the base temperature of the limiter was kept between 200°C and 300°C at all times. The beryllium limiter was inertially cooled during discharges and had an actively cooled baseplate to remove heat between discharges.

The beryllium limiter was installed at the top of the machine, acting as a rail limiter.

Up to the introduction of beryllium, ISX-B operated with titanium carbide coated graphite limiters, the walls of the vessel being stainless steel, sometimes gettered by titanium and for a short period by chromium. The reference discharges for the assessment of the beryllium limiter were made with the TiC limiter and without gettering. A set of standard parameters was established with plasma major radius 94cm, minor radius 24cm, elongation ≤ 1.2, toroidal field 1.4 T, plasma current 120kA, average electron density $4.5 \times 10^{19} m^{-3}$, electron temperature $\sim$700-800eV and injected power 0.8MW. The operational envelope was surveyed by scans of plasma density and current; at the same time, spectroscopic measurements were carried out to assess the impurity behaviour.

2. Limiter performance and heat loads for the different conditions of operation

The beryllium limiter was mainly studied under three conditions:

a. ungettered discharges

During the first three weeks of operation, about 800 shots were performed with ohmic heating only. Power fluxes to the limiter of 400-900W/cm^2 caused surface temperature rises of 100-200°C, and no damage to the limiter was observed.

For the remainder of the experiment, in addition to the ohmic heating, the plasma was heated by neutral injection. With power loads on the limiter up to the design load of 2.5 kW/cm^2, daily still photography of the limiter did not reveal any damage either.

During the first phase of the experiment, the plasma behaviour was dominated by the wall. Due to the high power losses by radiation from impurities coming from the wall, the specified temperature rise of 600°C for the limiter surface could not be achieved with the parameters chosen for the load test (power flux of 2.5kW/cm^2; plasma current of 120kA).

A current scan up to 165kA revealed that the power deposited onto the limiter increased with the plasma current. With current exceeding 140kA, power fluxes of 4-5kW/cm^2 were measured and the limiter surface showed signs of melting. Some cracks were observed on the limiter surface and a few chips spalled off the centre tiles (see Fig. 5-a). Reducing the power flux to the design load again caused no further limiter melting.

b. discharges with limiter surface melting

In order to reduce the effects of the wall on the plasma, it was decided to raise the power load on the beryllium limiter to melt its surface and to cover the walls with beryllium.

In the course of a prolonged series of high power discharges at a fixed plasma current (150kA), the power flux to the limiter was increased from 2.2kW/cm^2 to values exceeding 4kW/cm^2. The limiter surface melted and evaporation of beryllium caused strong gettering of the vacuum vessel. Fig. 5-b shows the damage done to the limiter surface by melting after 500 such discharges. During the shots where melting occurred, plasma operation was possible but not very reproducible.

c. gettered discharges

The power flux was then reduced to the design load again (2.5kW/cm^2). Because of the roughness of the limiter surface, the power flux was high enough at solidified droplets and protrusions to melt the surface locally. This resulted in beryllium evaporation, which gettered the walls sufficiently. Even with the limiter surface damaged, the discharges were good and reproducible. About 2000 shots were performed under these conditions (fluence test). There was no further gross melting and the surface topology was mainly preserved throughout the fluence test. Towards the end of the test, the features became somewhat finer due to evaporation and probably surface cracking (see Fig. 5-c).

Half of the limiter tiles were tesselated (as shown in Fig. 5-a) to reduce surface stress. Post-mortem analysis of the limiter tiles revealed that the tesselations had been quite successful in reducing surface stresses. While the non tesselated tiles show (as expected) surface cracks up to several millimeters deep, the tesselated ones show considerably less cracking. The total weight loss of the limiter, mostly in form of molten droplets, was 2g compared to a total weight of 3kg.

3. Impurities

a. ungettered discharges

For ohmic discharges as well as for low current beam discharges, the main impurity source was the wall and not the limiter. The beryllium content in the plasma was negligible (0.07% at the centre corresponding to a density of $4 \times 10^{16} m^{-3}$). The impurity content was dominated by oxygen, carbon and nitrogen with concentrations of about 1% each. The total Z_{eff} from hydrogen and light impurities was 2.4. The contribution from metals was only a few tenths; the titanium and chromium content of the plasma appeared to be 4 times smaller than that observed during operation with the TiC limiter.

b. discharges with limiter surface melting

For discharges with limiter surface melting, the radiated power dropped from 300kW to 150kW at constant plasma current (150kA) and density. The beryllium line intensities increased by factors of 15 to 300. The beryllium content in the plasma could reach values of about 5%. At the same time, radiation from light impurities decreased, indicating that beryllium was very effective in gettering the walls. The central radiation of C and O fell by factors of 2 to 4. Radiation from peripheral ions decreased by a factor of about 10. Fig. 6 illustrates for Be IV and O VI radiation the differences between ungettered and gettered discharges.

c. gettered discharges

Throughout the fluence test and during the post-fluence test, the beryllium influx was comparable (only a factor of 2 lower) to that observed for the discharges with limiter surface melting. The beryllium content in the discharge was about 2%. Because of its low atomic number (Z=4), beryllium does not contribute significantly to the plasma radiation. This is demonstrated very clearly in Fig. 7 which shows the total radiation together with the Be I and O VI radiation. Although the beryllium influx at the limiter increases drastically during the discharge, the total radiation seems to be dominated by the oxygen radiation, even though the oxygen content in the plasma is less than 0.5%.

Table V gives a comparison between the intensities of a few impurity lines for different conditions of operation of ISX-B. Note in particular that during the post-fluence test the oxygen radiation was considerably reduced compared to its level when TiC limiters were used.

4. Plasma behaviour

a. density limit

In ohmic discharges, the plasma performance in the presence of the beryllium limiter was much the same as with the TiC-coated graphite limiters. This is shown in the Hugill diagram (open and full squares in Fig. 8). The density limit was $6 \times 10^{19} m^{-3}$ for a plasma current of 170kA.

Scans obtained with additional heating (neutral beam injection) before properly gettering the walls are shown in Fig. 8 (full circles and open triangles). In particular, the density scan for a 116kA plasma current indicates that the plasma performance was comparable to previous data obtained with TiC limiters. The density limit was $9 \times 10^{19} m^{-3}$.

When the limiter surface melted during the shot, the discharges were not very reproducible and it was difficult to make a full density scan (crosses in Fig. 8). The highest electron density investigated was $9 \times 10^{19} m^{-3}$ for a 150kA plasma current.

With well gettered walls and a plasma current of 116kA, a maximum electron density of $1.3 \times 10^{20} m^{-3}$ was achieved before disruption (open circles in Fig. 8).

In ISX-B, beryllium gettering made it possible to reach density limits about 50% larger than titanium gettering and about 20% lower than chromium gettering. It should be emphasized here that the measurements were performed under different experimental conditions for the three investigated getter materials: evaporators were used to getter the walls either with titanium or chromium; during the chromium experiment, pump limiters with a gas flow rate of about 20 $torr.l.s^{-1}$ were also operational; beryllium gettering was done by merely melting the limiter. Thus it cannot be concluded that there is a significant difference in the density limit obtained with the three materials investigated.

b. Confinement

In the case of pure ohmic heating, the energy confinement time was 15ms for an electron density of $6 \times 10^{19} m^{-3}$ and a plasma current of 170kA. This value is comparable to the previous measurements made with TiC limiters.

Typical values of the energy confinement time τ_E measured with neutral beam heating in beryllium gettered discharges are plotted in Fig. 9 against the mean plasma density n_e.

The majority of the τ_E values measured under these conditions are independent of n_e and in good agreement with the empirical scaling found in ISX-B for gettered discharges: $\tau_E = \tau_E^{ISX}$.

However, a small number of these measurements exhibit a density dependence and are observed to approach the empirical scaling found in ungettered discharges and in gettered discharges with controlled neon puffing (the so-called Z-mode). This improvement in confinement is attributed by the ISX-B team to an outward radial shift of 1-2 cm in the plasma position /14/.

After careful analysis of the data for the beryllium gettered discharges, it can be concluded that beryllium gettering is similar in its effects on confinement compared to titanium and chromium gettering.

5. Conclusion

As far as we can conclude from the results of ISX-B experiments, beryllium is a prime candidate as a limiter and getter material for JET:

- its contribution to the plasma radiation is negligible, even at high concentrations, due to its very low Z value.

- it is an excellent getter material; its gettering efficiency is similar to that of titanium and chromium, when considering the plasma performance.

- the limiter has successfully withstood the specified fluence and load tests. In addition, thousands of reproducible plasma shots could be performed with the limiter, the surface of which was very rough after intentional melting.

V JET MAINTENANCE WITH BERYLLIUM

1. Introduction

Beryllium is one of the industrial materials (such as asbestos and sandblast debris) for which precautions must be taken against inhalation when they are present as airborne dust. This section explains how the JET vessel can be entered safely to carry out hands-on maintenance when there is a possibility that fine beryllium dust or lightly activated dust has been produced by plasma action. When tritium is also used, all maintenance within the Torus Hall will be executed remotely.

2. Inside the vacuum vessel

It is of paramount importance to the operation of JET that the surfaces forming the vacuum envelope remain absolutely clean, to a level at which molecular quantities are significant. Stringent precautions prevent contamination by people and tools when the vessel is opened. The vessel is entered through an access cabin with a changing room, entering air is filtered, and finally the walls are washed with high pressure demineralised water. It is intended that in future the flow of air into the torus will be minimised by supplying breathing air to the 3 to 6 operators by using air blouses with airlines as shown in Fig. 10, which are light, comfortable and easy to work in.

By the time beryllium is introduced the present access cabin will have been replaced by one illustrated in Fig. 11, which is sealed onto the pumping chamber, contains a personnel access lock and showers and provides the services, air, light, power and communications. The cabin will ensure cleanliness of the vessel and prevent migration of dust in either direction.

In the event that beryllium or active dust contamination is high enough to require precautions, the vessel will be washed with demineralised water, as at present, and wet vacuum cleaned. It might also be vented with steam before it is opened, to produce condensation which will damp down any dust, but the windows cannot at present tolerate water.

Air blouses are readily available and widely used for cleanliness in the pharmaceutical and electronics industries and as protection against airborne dust in others. A probably acceptable average level of airborne beryllium during an 8 hour shift would be about 2 mg/m^3. During entry and throughout the operations the air in the torus and in the various areas of the access cabin will be monitored by drawing known samples through filters and analysing the residue in an atomic absorption spectrometer. Results could be obtained every 30 minutes from any monitor. A static filter and mouthpiece are built into each blouse, for short-term safety in emergencies. Operators will carry monitors inside their blouses, close to their emergency filters. Protection from contact and inhalation of lightly activated dust or of beryllium dust is the same except for the monitoring methods. Radioactivity can be detected immediately.

Surface contamination will also be monitored in the torus and in the various areas of the access cabin. This is not important in the torus since the operators will in any case be completely covered. Beryllium firmly attached to the surface represents no hazard, although it could be removed by dilute nitric acid. Operators will wash down their outer garments in the access cabin and post them out to be cleaned and re-used or discarded.

If conditions should ever require them full suits, as Fig. 12, could be used.

There is no intention to clean up the inside of the torus in order to declare it an area for working with no protection, or to provide ventilation at 20 changes per hour, as required for direct breathing. The greater throughflow might carry dust and would require larger filters which in turn need to be disposed of.

3. Using the articulated boom

An existing overhead rail and travelling hoist can be passed in pieces through the entry cabin and erected inside the torus to carry and position heavy components.

If monitoring shows contamination levels to be sufficiently low, the articulated boom could be used instead, through the port opposite to the entry cabin. Contamination of the boom itself should be insignificant; it will not touch the walls and it is designed so that it can be washed as it is withdrawn. As an extra guarantee against any risk of spreading contamination beyond the boom support rail area, a local PVC enclosure can be set up.

4. Peripheral equipment connected to the torus

Experiments with beryllium in the UNITOR tokamak at the University of Dusseldorf and in the ISX-B at Oak Ridge show that transfer of beryllium into the vacuum circuit will be trivial and probably negligible. Monitored temporary enclosures, tents and bags were used successfully in both cases and can be used similarly on JET components if the vacuum circuit is breached at a point other than an entry point.

The neutral injection boxes and some of the diagnostics are identified as areas where these techniques must be carefully planned and proved in advance.

5. In the Torus Hall

With any possible contamination confined to the torus, or at worst to the access cabin or temporary enclosures, work on components having no connection with beryllium can continue in the Torus Hall with no precautions other than routine air monitoring.

6. Contaminated material

Materials which may have been contaminated will be washed in the lined operating box of the access cabin, then bagged and disposed of. The cabin can be sealed off and used for this and preparatory work while in the Assembly Hall. Large, new or decontaminated components will be passed directly through a roof hatch. If contaminated they could be passed through using bagging techniques.

7. Extra time and personnel needed for maintenance of the vacuum vessel with beryllium

The intended sequences of operations in sending personnel safely into the vacuum vessel are listed in Appendix I. The entry into and the exit out of the torus requires about 35 hours, when it is contaminated by beryllium dust, and around 22 hours, when it is not contaminated. This represents an extra time of 13 hours. To this figure must be added the two days of continuous washing of the vessel to remove beryllium dust before entry, which brings the total extra time to 61 hours. Taking into account the lack of experience at the beginning, one working week extra would be needed for the shutdown in order to have access safely into the torus containing beryllium dust.

One or two supplementary men are needed to look after the operations. An increase of 20% of the teams which enter the torus should be envisaged, to take into account the time lost in changes and showers.

VI CONCLUSIONS

The relative merits of beryllium and graphite as material for the JET limiters and wall have been discussed in length in this report. They can be summarised as follows:

- As beryllium has a lower Z-value than carbon, the total radiation losses are between 2 and 3 times smaller with beryllium than with carbon at the same concentration of impurity ions. However, in both cases, these losses remain low compared to conduction losses in the centre. Nevertheless, in the recent JET experiments with graphite limiters and carbonised walls, it has been observed that a large fraction of the radiated power at the edge is due to carbon and oxygen.

- Beryllium has a negligible porosity and a lower yield on sputtering by hydrogen compared to graphite. At the actual temperatures of the JET belt limiters, the hydrogen retention is 2-3 times lower in beryllium than in graphite. After heating at 800°C, the graphite tiles of the belt limiter could release between 2 and 8×10^{19} hydrogen atoms $/m^3$ on average. This might make density control difficult.

- The thermomechanical properties of beryllium do not appear as good as those of graphite; in particular, surface melting of the beryllium limiter could occur in the case of a severe heat overloading. However, the series of tests carried out at Sandia National Laboratory and in ISX-B have shown that these properties are suitable for JET. In ISX-B, even after melting the limiter surface by intentional heat overloading, its structural integrity was preserved and thousands of reproducible discharges could be performed. For a total input power of 40MW in JET, the beryllium belt limiter will be designed with a safety factor of 1.4 with respect to melting, taking for local peak loads an upper limit imposed by the evaporation rate.

- On best knowledge beryllium is the only low-Z element which can be used as a structural material for limiters and which also acts as an excellent getter. Beryllium is then the best candidate to reduce radiated power losses in the centre as well as at the edge of the plasma, if used as a material for the limiters and wall.

- The main drawback of beryllium is the toxicity of its dust. However, the control of beryllium dust is well within standard industrial techniques. This should be even simpler in JET, because it is a closed system conceived to operate with tritium.

It should be possible to use graphite limiters covered by a thin beryllium layer, but the behaviour of such limiters is still not known (e.g.beryllium carbide formation, melting of beryllium on the graphite surface, which would be heated above the melting point of beryllium). Thus beryllium appears to offer the best prospects as a material for the JET limiters and wall. If gettering is not needed and if the density can be easily controlled, the use of graphite limiters could also be a good solution.

Acknowledgements: The authors are very grateful to Drs R Bickerton, W Engelhardt and P Stott for stimulating discussions and useful criticisms. They also thank Dr B E Keen for a careful reading of the typescipt.

REFERENCES

/1/ The JET Project - Design Proposal - Report of the Commission of the European Communities, EUR 5516e (EUR-JET-R5) (1976)

/2/ Rebut PH and Hugon M, in Plasma Physics and Cont. Nuc.Fusion Res. (Proc. 10th Int. Conf., London, 1984) 2, IAEA, Vienna (1985) 197

/3/ Rebut PH and Green BJ, in Plasma Physics and Cont. Nuc. Fusion Res. (Proc. 6th Int. Conf., Berchtesgaden, 1976) 2, IAEA, Vienna (1977) 3

/4/ Vernickel H and Bohdansky J, Nuclear Fusion 18 (1978) 1467

/5/ Watkins ML and Abels-van Maanen AEPM, Proc. 11th Eur. Conf. on Cont. Fusion and Plasma Physics, Aachen, 1983, 2, EPS (1983) 303

/6/ Watkins ML et al, J. Nucl. Mater. 121 (1984) 429

/7/ Sevier DL et al, J. Nucl. Mater. 103, 104 (1981) 187

/8/ Wolfer WG et al, J. Nucl. Mater. 111, 112 (1982) 560

/9/ Roth J et al, J. Nucl. Mater. 111, 112 (1982) 775

/10/ Bohdansky J et al, Report on Sputtering Measurements of Beryllium, IPP-JET No 31 (1985)

/11/ Doyle BL et al, J. Nucl. Mater. 103, 104 (1981) 513

/12/ Möller W et al, Retention and Release of Deuterium Implanted into Beryllium, IPP-JET No 26 (1985)

/13/ JET Beryllium Limiter Test on ISX-B, Reports of January to December 1984

/14/ Wootton AJ, Bush CE, Edmonds PH, Lazarus EA, Ma CH, Murakami M and Neilson GH(1985), to be published

SYMBOL KEY TO TABLES I AND II

$\hat{T}_i$	Central ion temperature
$\hat{n}_{DT}$	Central deuterium/tritium density
$\hat{Z}_{eff}$	Central effective ionic charge
$\hat{f}_{low}$	Central ratio of low Z impurity and electron densities
$\hat{f}_{med}$	Central ratio of medium Z impurity and electron densities
$\bar{\tau}_E$	Global energy confinement time
$\bar{n}_e$	Volume averaged electron density
$n_{e(lim)}$	Electron density at limiter tip
$T_{i(lim)}$	Ion temperature at limiter tip
$T_{e(lim)}$	Electron temperature at limiter tip
P_{in}	Net input power from radiofrequency heating (15MW), neutral beam injection heating (17.25MW, Table II; 15MW, Table IV) and ohmic heating - Prompt charge exchange losses from the neutral beam
P_α	Alpha Power
P_{rad}	Radiated Power
P_{lim}	Parallel Transport Power to the limiter
P_{wall}	Perpendicular Transport Power to wall
P_{neut}	Charge-exchange and Ionisation Power
$\dot{W}$	Rate of increase of plasma energy
S_{low}	Rate of erosion of low Z material
S_{med}	Rate of erosion of medium Z material

TABLE I

Limiter/Wall	Be/Be	C/C	Be/Ni	C/Ni
$\hat{T}_i$ (keV)	9.8*	9.8	8.7	8.5
$\hat{n}_{DT}$ ($x10^{19}m^{-3}$)	10.8	10.9	10.2	10.2
$\hat{f}_{low}$ / $\hat{f}_{med}$ (%)	.5/0	.5/0	.3/.1	.3/.1
$\hat{Z}_{eff}$	1.1	1.1	1.7	1.7
$n_{e(lim)}$ ($x10^{19}m^{-3}$)	1.5	1.3	0.72	0.66
$T_{i(lim)}$ (eV)	181	206	39	40
$T_{e(lim)}$ (eV)	229	246	21	20
$\bar{n}_e$ ($x10^{20}m^{-3}$)	0.59	0.57	0.51	0.50
$\bar{\tau}_E$ (s)	1.1	1.0	0.6	0.6
P_{in} (MW)	26.6	26.5	29.6	29.7
P_{α} (MW)	5.6	5.5	3.4	3.2
P_{rad} (MW)	1.1	1.3	32.9	32.8
P_{lim} (MW)	19.5	18.9	0.6	0.5
P_{wall} (MW)	2.3	2.6	.6	.7
P_{neut} (MW)	3.5	5.3	.4	.3
$\dot{W}$ (MW)	5.8	3.9	- 1.5	- 1.4
S_{low}/S_{med} ($x10^{22}$ particles/s)	.6/0	.4/0	.02/.1	.04/.1

*$\hat{T}_i$ still increasing at time, t=3s.

TABLE II

Limiter/Wall	Be/Be	C/C	Be/Ni	C/Ni
$\hat{T}_i$ (keV)	12.8	11.3	10.9	9.9
$\hat{n}_{DT}$ ($x10^{19}m^{-3}$)	6.0	5.8	6.0	5.8
$\hat{f}_{low}$ / $\hat{f}_{med}$ (%)	3.7/0.0	3.1/0.0	3.5/.09	2.7/.1
$\hat{Z}_{eff}$	1.4	1.9	2.0	2.4
$n_{e_{(lim)}}$ ($x10^{19}m^{-3}$)	.68	.84	.68	.82
$T_{i_{(lim)}}$ (eV)	107	132	128	133
$T_{e_{(lim)}}$ (eV)	202	170	172	148
$\bar{n}_e$ ($x10^{20}m^{-3}$)	·42	·43	·44	·44
$\bar{\tau}_E$ (s)	.71	.56	.51	.44
P_{in} (MW)	25.4	26.2	26.7	27.1
P_{α} (MW)	2.5	1.8	1.7	1.4
P_{rad} (MW)	.7	.9	10.1	10.1
P_{lim} (MW)	19.0	20.2	13.5	14.4
P_{wall} (MW)	2.6	2.2	.2	.2
P_{neut} (MW)	1.1	1.1	.2	.3
$\dot{W}$ (MW)	4.5	3.6	4.4	3.5
S_{low}/S_{med} ($x10^{22}$ particles/s)	1.4/0.0	1.1/0.0	.8/.09	.7/.08

*$\hat{T}_i$ still increasing at time, t=3s.

TABLE III

	Be	graphite
Z	4	6
density (g/cm^3)	1.85	1.6-1.85
porosity	$\cong 0$	18% - 28%
electrical resistivity ($\mu\Omega.cm$)	0.03	11.4
heat of evaporation (J/mol)	3.10^5	7.10^5
melting point	1277°C	-
boiling/sublimation point	2770°C	4450°C
k, thermal conductivity ($W.m^{-1}.K^{-1}$)	120	70
c, specific heat ($J.kg^{-1}.K^{-1}$)	2700	1500
α, thermal expansion coefficient ($^oC^{-1}$)	$13x10^{-6}$	$5x10^{-6}$
E, elastic modulus x 10^{-5} ($N.mm^{-2}$)	3-1	0.13
σ_B,ultimate tensile strength ($N.mm^{-2}$)	300-100	50
ductility (% elongation)	4-50	

TABLE IV

	Be			C		
Peak load (W/cm^2)	300	400	500	300	400	500
$T_S(^oC)$ at the end of each pulse	740	920	1120	1050	1310	1610
$T_S(^oC)$ at the start of each pulse	280	280	280	280	280	280

TABLE V

Ion	λ(Å)	TiC limiter	Beryllium Limiter		
			116kA no melting	155kA melting	116kA post fluence
Be I (L)	2348	–	17	430	357
Be II (L)	3131	–	300	4800	4288
Be IV	76	–	0.4	29	15.2
Cr XIII	328	1.5	0.35	0.70	~0.25
Ti XI (L)	386	7.0	2.35	~0.06	0.7
Ti XII	461	6.0	1.4	1.00	~0.4
Fe XVI	361	2.0	0.9	0.75	0.18
O VI	1032	450	300	30	8.5

CR 85.43

Absolute intensities of typical impurity lines. (L) denotes observation of the limiter.

APPENDIX I: DETAILED PROCEDURE FOR INTERVENING IN THE VACUUM VESSEL THROUGH OCTANT NO. 1

Intervention into the vacuum vessel includes three distinct phases: entry, work inside and exit. The successive operations for the three phases are listed below with their durations, when beryllium dust is present (column A) and absent (column B). The durations are given in hours.

Entry into the vacuum vessel	A	B
1. Vent the vessel to atmosphere. Possibly add steam to condense and damp down dust.		
2. Carry the access cabin (Fig. 11) into the Torus Hall by crane, with prepared equipment in the operating box.	1	1
3. Wheel access cabin into position so that the seal on the cabin mates with a flange on the pumping chamber door. Jacks controlled by a man on a platform adjust the cabin height.	½	½
4. Inflate pneumatic seal between cabin and flange and fit extensible PVC sleeve around it (Fig. 13).	½	0
5. Connect services to cabin, ie water (some at 80 bar for washing vessel), electricity, compressed air, television, intercom, and breathing air for air lines.	½	½
6. Switch on ventilation plant in cabin to produce about 5 mbar depression in operating box. Air is drawn through the change room and personnel lock and discharges back onto the torus hall through HEPA filters.	½	½

		A	B
7.	Connect operating box to pumping chamber by a flexible pipe containing a HEPA filter, to balance pressures. Check balance by flow meter.		
8.	Operators don protective clothing (plastic suits and air blouses with airlines) in the interspace between showers in the personnel air lock. Minimum of 3 operators.	½	½
9.	Open pumping chamber door, either on hinges or remove by hoist on operating box ceiling.	1	1
10.	Health physicist in full suit checks radiation level at and near the torus entry by radiation detectors, air dust samples and swabs.	2	1
11.	Additionally, if beryllium present, health physicists take air samples and swabs which are taken away for analysis.		
12.	Fit seal face protector on door flange and tape it to the face of the operating box. Fit a protecting tube inside the pumping chamber passage (to prevent things falling into the pumps) and lay staging along the bottom of the tube with a ladder extending down into the vessel.	1	1
13.	Plug in services leading below staging into the vessel.	½	½
14.	Health physicist enters vessel and monitors conditions.	2	1

Times are for each measurement: the operation will be repeated as deemed necessary.

		A	B
15.	Operators enter vessel and clean up contamination as and if necessary by:		
	a. Dry vacuum cleaners with HEPA filters	4	0
	b. Protecting windows and washing with high-pressure water followed by wet vacuum cleaning.	48	0

Work inside the torus

16. Progressively extend lighting, TV cameras, microphones and other services.

17. Proceed with work in vessel. Wearing air suits will not restrict the period over which a man can work without a break. Other factors would impose the limit. These suits, with fresh air cool or warm, are found to be very comfortable.

    Care must be taken as pockets which may contain beryllium dust are exposed when components are removed: they can be washed as they are exposed. Cutting and welding could release beryllium bonded to surfaces: debris must be drawn off by vacuum cleaners into filters.

18. Contaminated components and materials will be passed into the operating box where they can be washed, bagged if necessary, and posted via the waste drum.

    Some bench work may be done in the operating box.

		A	B
	Exit from the vacuum vessel		
19.	When work is finished, progressively dismantle equipment and carry it back into the operating box, cleaning up the vessel and water washing in the same way as at present.	8	8
20.	Re-install the pumping chamber door and wipe down all the surfaces as far as the pneumatic seal (Fig. 13).	6	4
21.	Remove the pressure balance pipe, with filter.	½	½
22.	Pump down the vacuum vessel and test the door for leaks. Re-fit until satisfactory.		
23.	Withdraw cabin until PVC sleeve is extended.	2	0
24.	Crimp weld and cut the sleeve (Fig. 13, broken lines).		
25.	Fit a closure lid over the PVC bag stub on the cabin. The stub remains in position until the next intervention.	½	0
26.	At convenient times while the services are connected, personnel may leave the operating box through the personnel air lock which contains 2 showers. They doff their suits between the 2 showers and post them out for decontamination and re-use or disposal.	½	½
27.	Take away the cabin which can be connected to services elsewhere so that further work and cleaning up can continue.	1	1

		A	B
28.	Remove the PVC bag stub from the pumping chamber (Fig. 13, broken line), using vacuum cleaners with HEPA filters, washing down, air monitoring and taking swabs, all under health physics supervision. Access to the Torus Hall must be restricted.	2	0
29.	Normal operating conditions are restored.		
	- Total times assuming single monitoring operation at item 14 and excluding washing at item 15b:	34½	21½
	- Washing at item 15b:	48	0

If it is necessary to have access also in the torus through Octant No. 5, 6 extra hours (3 for item 2 and 3 for item 27) should be needed to carry the intervention module in two sections over the neutral beam injector.

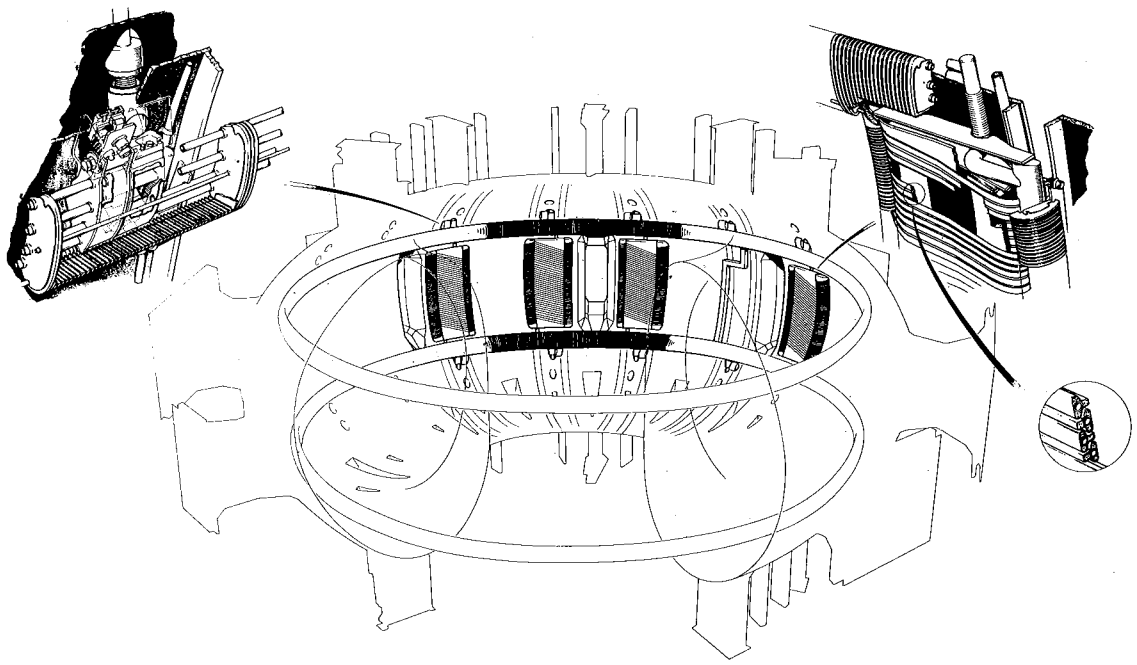

Fig. 1 Antenna and Toroidal Limiter.

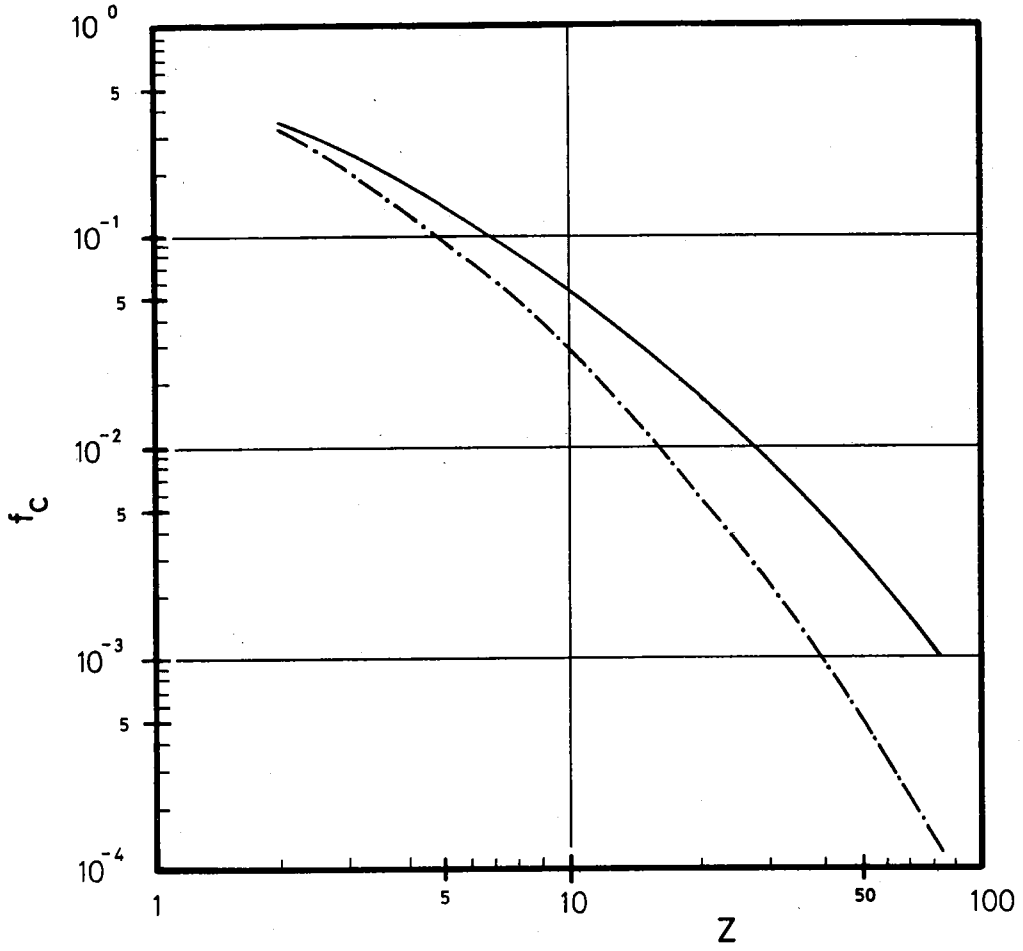

Fig. 2 Critical impurity concentration f_c as a function of atomic number Z for two electron temperatures (———: T = 35 keV; —·—·—·—: T = 12 keV). For Z < 6, radiation loss was considered to be bremsstrahlung only (see Ref./4/).

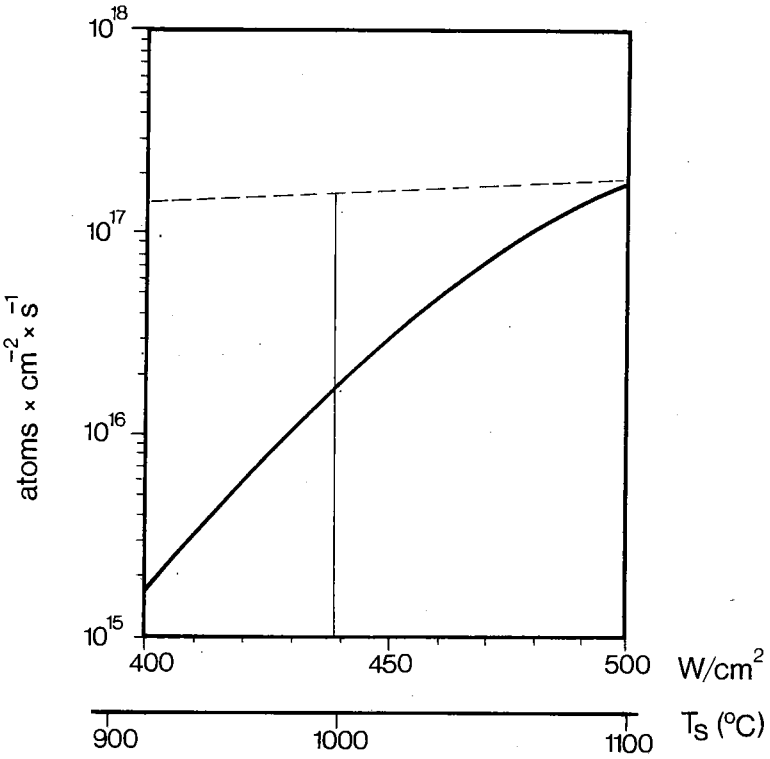

Fig. 3 Evaporation rate (full line) and sputtering rate (dotted line) of beryllium as a function of temperature.

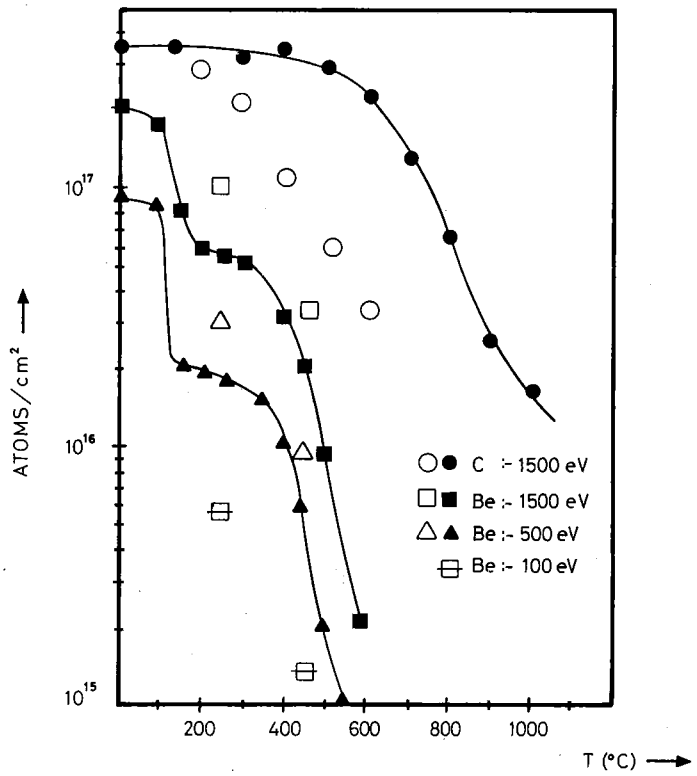

Fig. 4 Hydrogen retention as a function of temperature. The full symbols are the data obtained for implantation at room temperature and a subsequent heating to the temperatures indicated on the graph. The open symbols correspond to the results obtained for implantation at the temperatures indicated on the graph.

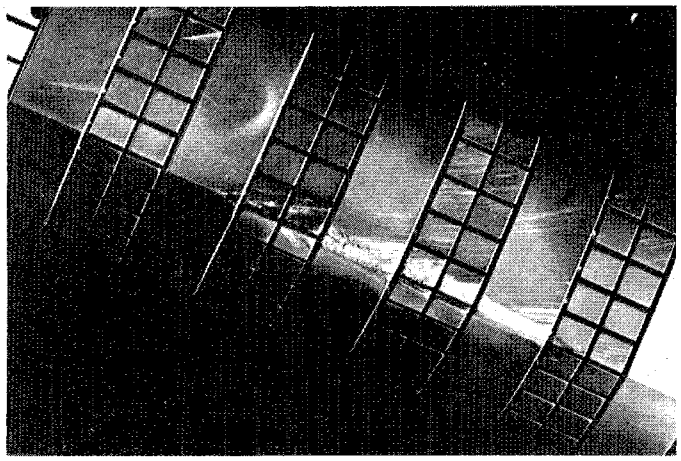

a)

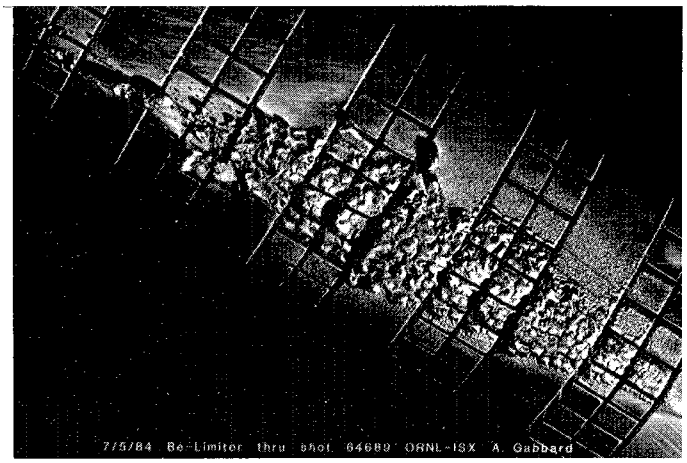

b)

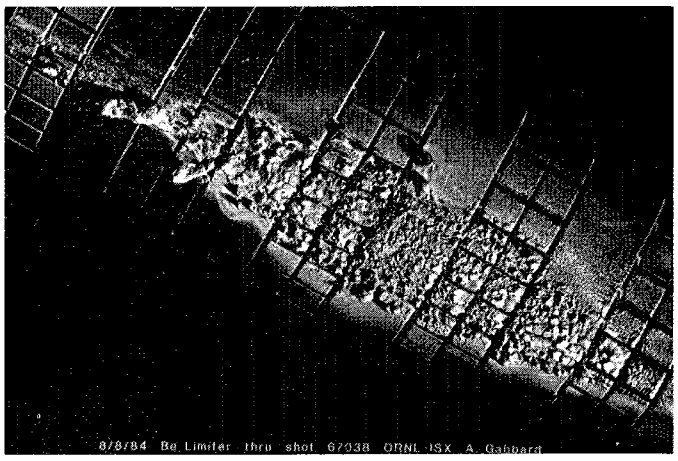

c)

Fig. 5 Surface structure of beryllium limiter after:
(a) a few shots with power fluxes exceeding 4 kW/cm^2
(b) melting
(c) the fluence test.

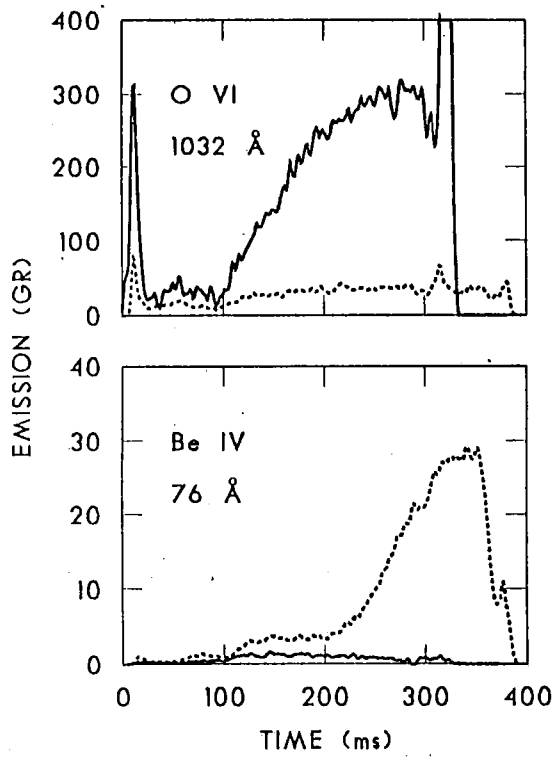

Fig. 6 Temporal behaviour of beryllium and oxygen radiation for ungettered discharges at 116kA (solid curve) and gettered discharges at 150kA (dashed curve). The injected beam power is 0.85MW.

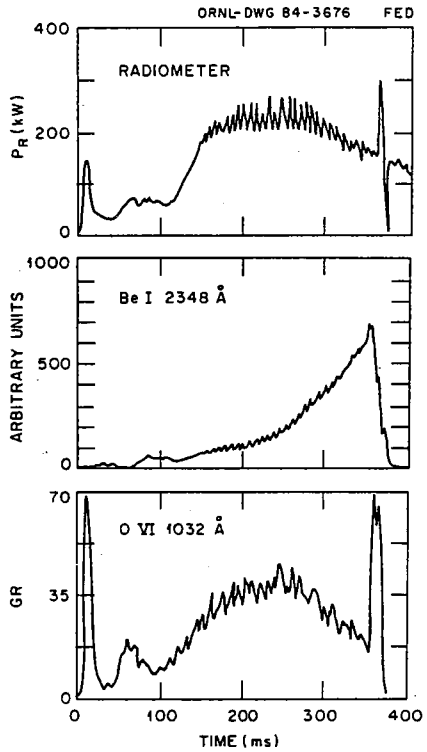

Fig. 7 Temporal behaviour of total radiation, Be I radiation at the limiter, and OVI radiation. The plasma current is 116kA and the beam heating power is 0.85MW.

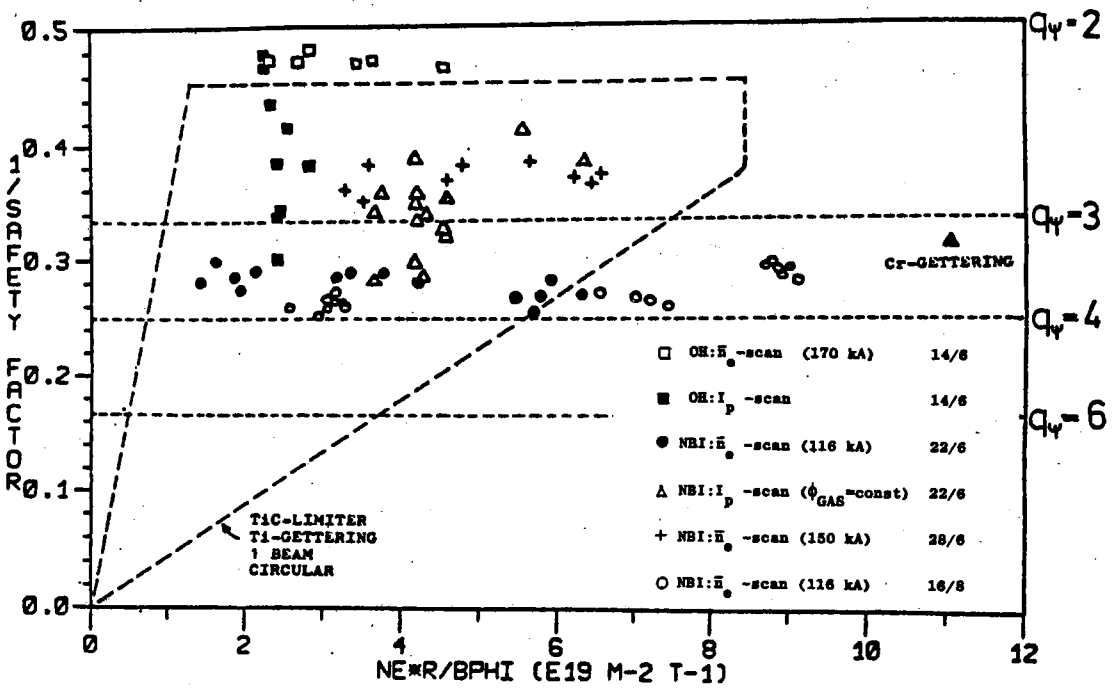

Fig. 8 Hugill Diagram with beryllium in ISX-B (see text).

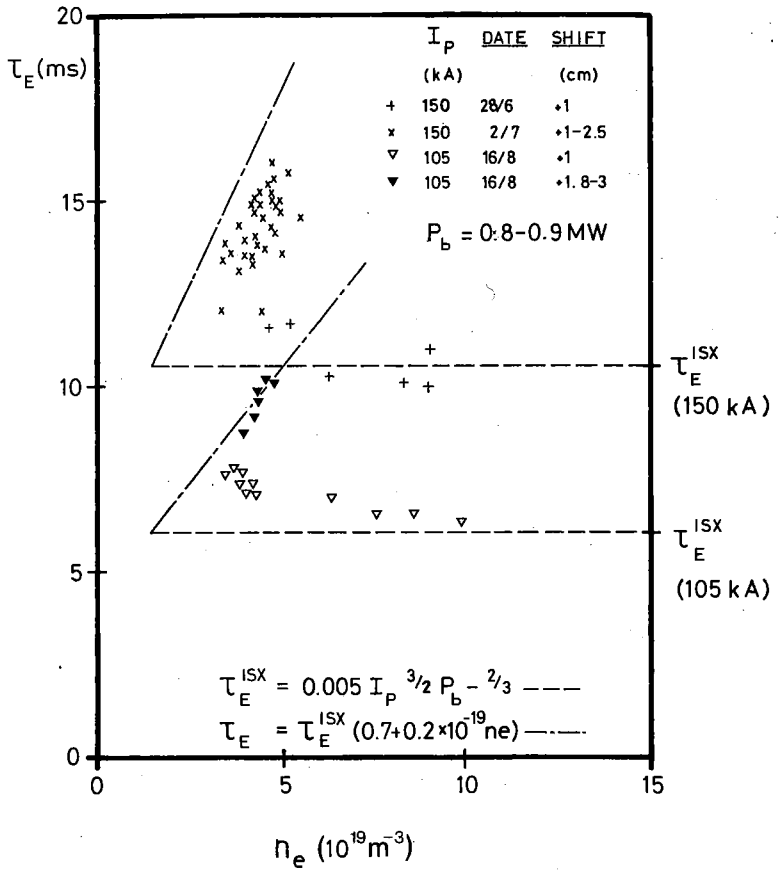

Fig. 9 Density scans of energy confinement time for the beryllium experiment in ISX-B.

Fig. 10 Typical air-blouse. Can use airline in place of filter/power unit shown.

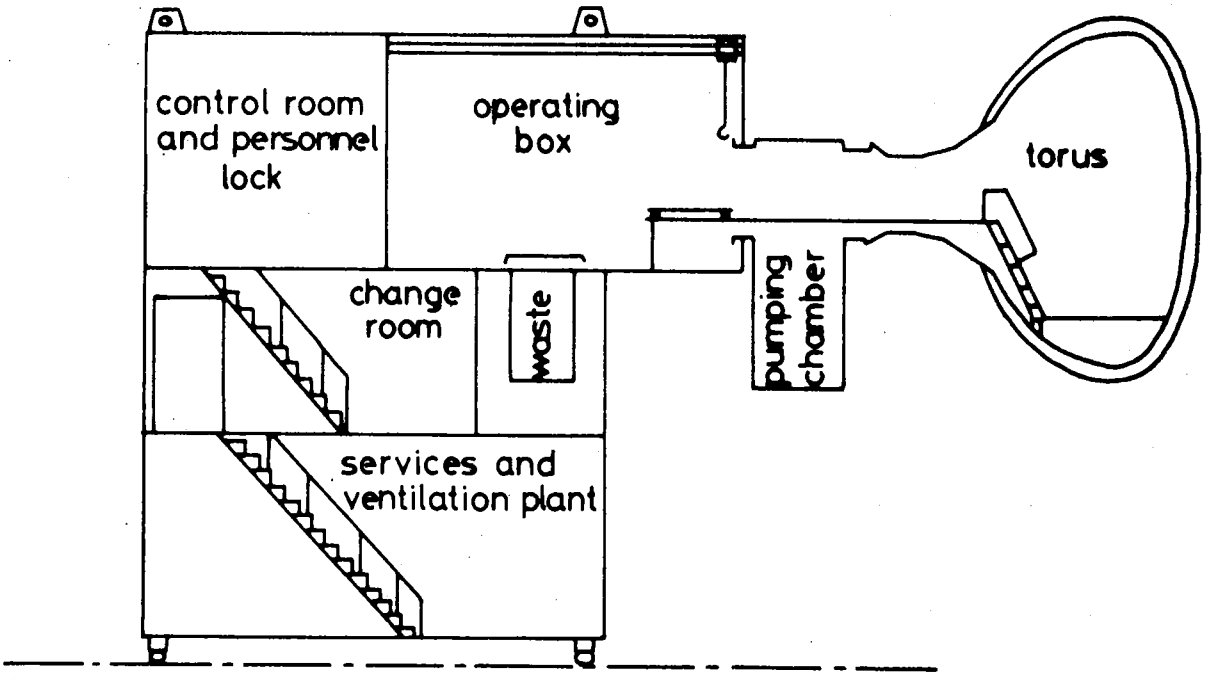

Fig. 11 Torus access cabin.

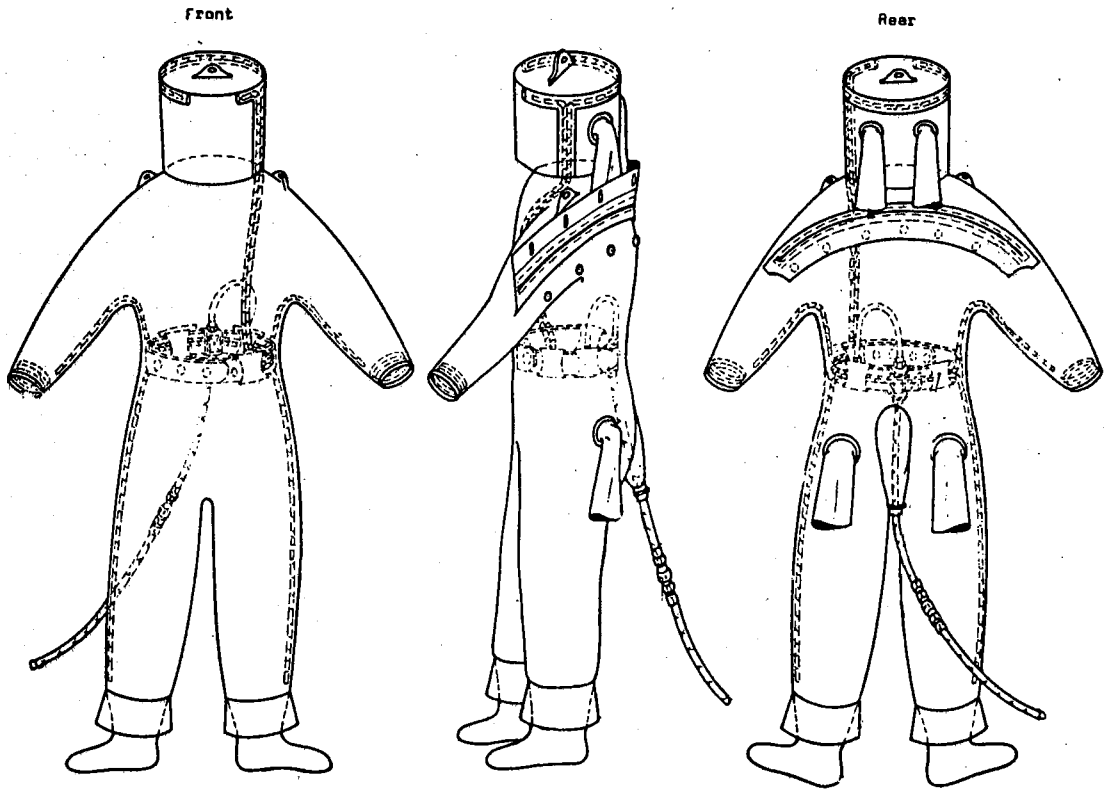

Fig. 12 Typical full air suit.

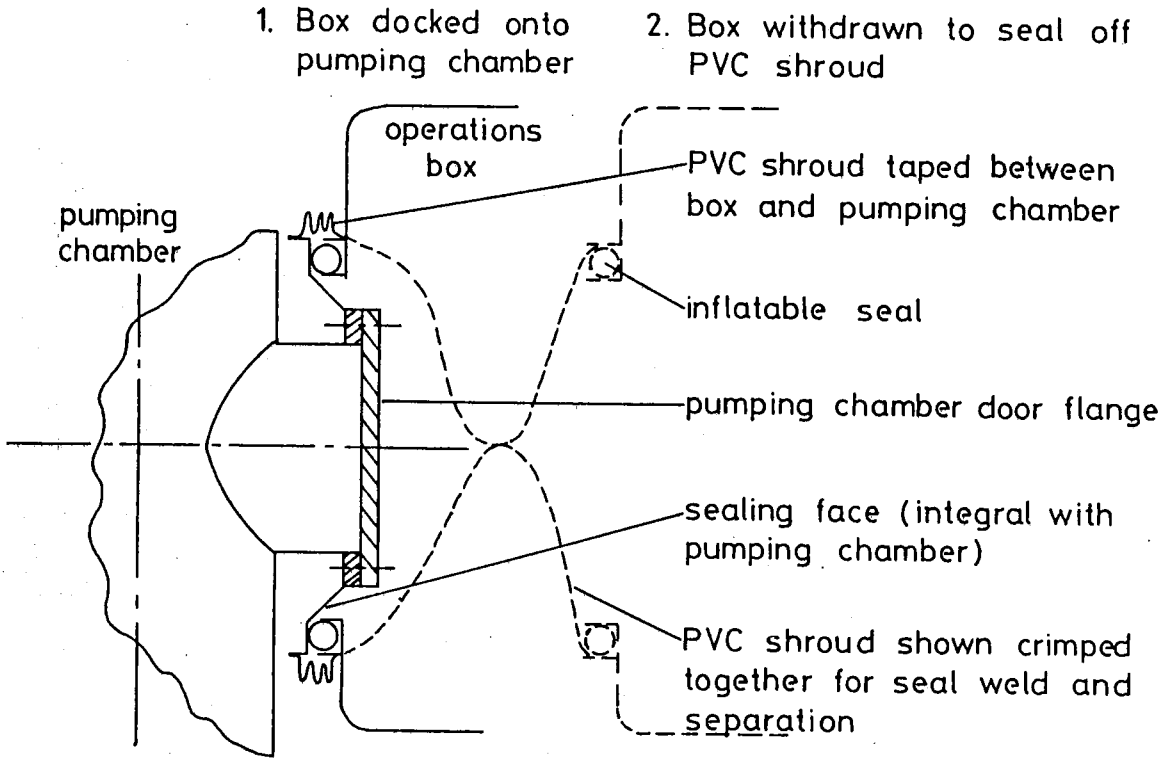

Fig. 13 Access cabin docked onto pumping chamber.